Bone 179 (2024) 116973

Contents lists available at ScienceDirect

Bone

journal homepage: www.elsevier.com/locate/bone

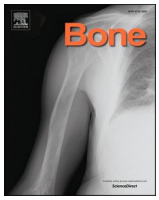

Full Length Article

A comparison of bone microarchitectural and transcriptomic changes in murine long bones in response to hindlimb unloading and aging

Steven J. Meas [a], Gabriella M. Daire [a], Michael A. Friedman [a], Rachel DeNapoli [a], Preetam Ghosh [a], Joshua N. Farr [b], Henry J. Donahue [a,*]

[a] Virginia Commonwealth University, Richmond, VA 23284, USA
[b] Mayo Clinic College of Medicine, Rochester, MN 55905, USA

ARTICLE INFO

Keywords:
Disuse
Hindlimb unloading
Aging
Senescence
Transcriptomics

ABSTRACT

Age- and disuse-related bone loss both result in decreases in bone mineral density, cortical thickness, and trabecular thickness and connectivity. Disuse induces changes in the balance of bone formation and bone resorption like those seen with aging. There is a need to experimentally compare these two mechanisms at a structural and transcriptomic level to better understand how they may be similar or different.

Bone microarchitecture and biomechanical properties were compared between 6- and 22-month-old C57BL/6 J male control mice and 6-month-old mice that were hindlimb unloaded (HLU) for 3 weeks. Epiphyseal trabecular bone was the compartment most affected by HLU and demonstrated an intermediate bone phenotype between age-matched controls and aged controls.

RNA extracted from whole-bone marrow-flushed tibiae was sequenced and analyzed. Differential gene expression analysis additionally included 4-month-old male mice unloaded for 3 weeks compared to age-matched controls. Gene ontology analysis demonstrated that there were age-dependent differences in differentially expressed genes in young adult mice. Genes related to downregulation of cellular processes were most affected in 4-month-old mice after disuse whereas those related to mitochondrial function were most affected in 6-month-old mice. Cell-cycle transition was downregulated with aging.

A publicly available dataset (GSE169292) from 3-month female C57BL/6 N mice unloaded for 7 days was included in ingenuity pathway analysis (IPA) with the other datasets. IPA was used to identify the leading canonical pathways and upstream regulators in each HLU age group. IPA identified "Senescence Pathway" as the second leading canonical pathway enriched in mice exposed to HLU. HLU induced activation of the senescence pathway in 3-month and 4-month-old mice but inhibited it in 6-month-old mice.

In conclusion, we demonstrate that hindlimb unloading and aging initiate similar changes in bone microarchitecture and gene expression. However, aging is responsible for more significant transcriptome and tissue-level changes compared to hindlimb unloading.

1. Introduction

Osteoporosis is a disease that is caused by low bone mineral density (BMD) and leads to an increased risk of fracture, with significant effects on morbidity and mortality. Osteoporosis increases in prevalence with age; hence the burden of osteoporotic fractures is predicted to increase as the global population ages [1,2]. Decreased mechanical loading, as observed in patients with limited mobility, e.g. patients with hip fractures, can result in disuse-related bone loss [3]. An emerging concept is that disuse induces physiological changes in bone similar to those seen with aging [3,4]. Age and disuse-related bone loss both result in decreases in BMD, cortical thickness, and trabecular thickness and connectivity [3]. This effect on bone reduces biomechanical strength and fracture resistance [5]. Whereas age-related bone loss progresses at a rate of about 0.17 % per month, disuse-related bone loss demonstrates an accelerated rate of bone loss at 1–2 % per month [4,5]. Several strategies (i.e. weight-bearing exercise and resistance training) have been employed to combat both age- and disuse-related bone loss, with

* Corresponding author.
E-mail addresses: meass2@vcu.edu (S.J. Meas), dairegm@vcu.edu (G.M. Daire), mafriedman@vcu.edu (M.A. Friedman), denapolir@vcu.edu (R. DeNapoli), pghosh@vcu.edu (P. Ghosh), farr.joshua@mayo.edu (J.N. Farr), hjdonahue@vcu.edu (H.J. Donahue).

https://doi.org/10.1016/j.bone.2023.116973
Received 17 September 2023; Received in revised form 15 November 2023; Accepted 16 November 2023
Available online 21 November 2023

limited effectiveness [6]. Hence, new strategies for preventing the progression of both types of bone loss are needed to promote healthy aging.

One of the hallmarks of age-related bone loss is cellular senescence; a process characterized by cell cycle arrest and distinct changes in cellular expression, metabolism, and secretion [7]. Senescent cells accumulate in aging tissues and establish a senescence associated secretory phenotype (SASP), which is associated with detrimental effects on tissue [7]. In bone, SASP is associated with an increase in osteoclastogenesis and bone resorption, especially evident following a marked increase in number of senescent osteocytes in mice older than 18 months [8–11]. These age-related changes are paralleled in models of disuse, where unloading causes increased osteoclastogenesis and activity, decreased osteoblastogenesis, and increased bone marrow adiposity [3]. Despite recent advances in the field of bone biology and senescence, there has been little consideration of senescence in the context of disuse-induced bone loss, despite parallels to age-related bone loss, including increased inflammation [12–14]. The few studies that have considered senescence in the context of disuse examined the vertebral column or musculature surrounding the long bones [15,16]. However, the long bones themselves, primarily the femur and tibia, are significantly affected by disuse-paradigms such as hindlimb unloading or single limb immobilization [17,18].

To date, the relationship between senescence, age- and disuse-related bone loss has not been directly examined, especially in terms of the transcriptome. This is a significant gap in understanding the mechanisms disrupting bone homeostasis and the onset of unloading-induced osteoporosis. We hypothesize that age- and disuse-related bone loss develop through similar mechanisms, including senescence. Herein, we aimed to examine the novel role of senescence in disuse-related bone loss, and to directly compare the phenotype in age- and disuse-related bone loss.

2. Materials and methods

2.1. Animal model

All animal procedures were approved by the VCU IACUC. Animal studies used 6- and 22-month C57BL/6J male mice (000664, Jackson laboratories). We wanted to choose skeletally mature mice that would parallel both young adult and old humans. 6-month and 22-month old mice are roughly equivalent to a 30 year old and 60 year old human, respectively [19]. Animals were received one month younger than their starting age to become accustomed to our institutional vivarium (i.e. 22-month mice were received at 21-months of age). They were allowed to acclimate in experimental cages one week prior to intervention. The disuse-related model of bone loss was established by hindlimb unloading (HLU) for 3 weeks, as has been performed extensively in our laboratory [18,20,21]. These experiments were performed using rat cages with a wire mesh bottom (Allentown) to allow for tail suspension. Under anesthesia, mice tails were wrapped with two strands of porous medical grade tape (3 M). The distal portion of the tape was attached to a steel eye hook, which was connected to string wrapped around an elevated crossbar. The line was rotated, elevating the tail and hindlimbs of the mouse until the hindlimbs formed an angle of 30° with the ground. This set-up provided mice free access to food and water within a restricted navigable area. If mice lost >10 % body weight, they were supplemented with DietGel Boost (ClearH2O). Mice were euthanized if humane endpoints were reached (loss in body weight > 20 %, open-ulcers), and those mice were excluded from the study. Animals were dual-housed. Control groups were housed in the same cage system except for tail-suspension. Power calculation predicted a sample size of 5 mice was needed per group. Total group numbers for mice included 6-month-old male control ($n = 8$), 6-month-old male HLU (n = 8), and 22-month-old male control ($n = 11$). A breakdown of groups can be found in Table 1. Rows indicate group, Columns indicate the type of analysis, and "Yes" indicates that this group was included in this type of analysis.

2.2. microCT parameters

Before and after HLU, mice femurs were scanned using X-ray micro computed tomography (SkyScan, Bruker). Animals were anesthetized using vaporized isofluorane and subjected to a scan of the femur at a resolution of 4032 × 3024 and 7 μm. Images were reconstructed in three dimensions and analyzed using software from the manufacturer (Bruker). A 180 μm section of the midpoint was isolated for cortical bone analysis. A 720 μm section was isolated proximal to the epiphyseal plate for metaphyseal trabecular bone analysis. A 520 μm section was isolated distal to the epiphyseal plate for epiphyseal trabecular bone analysis. The following cortical bone parameters were examined: bone mineral density, cortical area fraction, and cross-sectional thickness. The following trabecular bone parameters were examined: percent bone volume, trabecular thickness, trabecular number, and trabecular separation. Bone parameters were analyzed using final values and as a percent change from baseline. Percent change from baseline was calculated as follows; 100* (D20 – D0)/D0, where D0 refers to baseline measurements and D20 refers to measurements after the three week intervention period. Femurs were rescanned post-sacrifice if images could not be used for analysis, however samples were excluded from percent change from baseline calculations if baseline images were not clear. Bone mineral density was calibrated based on attenuation coefficients from samples with known density. Attenuation coefficient for 0.25 g/cm^3 was 0.019 cm^2/g, and 0.75 g/cm^3 was 0.036 cm^2/g. Samples for any of these parameters were excluded from analysis if computational results were beyond mean ± 2 standard deviations or if they contradicted empirical evidence.

2.3. Biomechanical testing

Mechanical properties of femurs were evaluated by three-point bending to failure under displacement control at 1.0 mm/min using Bose ElectroForce 3200, as previously described [17]. The following parameters were examined: yield load, ultimate load, yield displacement, work-to-fracture, yield stress, ultimate stress, post-yield strain and total toughness.

2.4. Transcriptomics

Distal and proximal ends of tibiae were removed prior to flushing out the bone marrow using a microcentrifuge. The remaining portion of the tibiae was stored in RNAlater (Sigma-Aldrich, R0901-500ML) overnight at 4 °C before removing solution and storing at −80 °C until ready for processing. Frozen bones were ground with a mortar and pestle in liquid nitrogen and bone dust was homogenized in bead mill tubes

Table 1
Summary of experimental groups.

Age (in months)	Group	microCT	Biomechanical Testing	RNASeq	Ingenuity Pathway Analysis	Reference
3	HLU & Control				Yes	Spatz et al., 2021
4	HLU & Control			Yes	Yes	Friedman et al., 2023
6	HLU & Control	Yes	Yes	Yes	Yes	This study
22	Control	Yes	Yes	Yes	Yes	This study

(FisherBrand, 15–340-151) in Trizol (Thermo Fisher, 15,596,026). RNA was extracted from bone-marrow flushed tibias from each group using RNEasy Mini Kit (Qiagen, 74,104) and samples with an RNA integrity number >4.0 were used for bulk RNAseq. RNAseq library was prepared (Illumina stranded mRNA prep) and performed on Nextseq 2000 P3–200 cycles (up to 1.1 billion reads) (Illumina). Paired-end raw sequence data was processed using BioJupies and analyzed using plug-ins for analysis [22]. This online tool uses the kallisto pseudoaligner to generate gene counts. Primary component analysis, clustergrammer [23] were performed on the top 2500 genes, using logCPM normalized values. Differential gene expression was powered using limma [24].

We also performed analysis of RNASeq data using Ingenuity Pathway Analysis (IPA) from Qiagen to determine whether "Senescence Pathway" is an upregulated Canonical pathway in HLU mice [25]. We included two additional datasets in our comparison analysis. First, 4-month-old C57BL/6 J male mice subject to HLU for a period of three-weeks from our recently published study, which included detailed analysis of bone geometry and mechanical properties [21]. Second, a dataset (GSE169292) from the NIH GEO which contained results from 3-month-old female C57BL/6 N mice subjected to HLU for a period of seven days [26]. A summary of experimental groups can be found in Table 1. IPA was performed using approximately the top 3000 molecules with lowest *p* values from differential gene expression analysis of control versus HLU in each age group. *P* values were calculated by the software based on logFC values using the Fisher exact test to determine if the "Senescence Pathway" was enriched. Benjamini-Hochberg procedure to correct for the false discovery rate was calculated by the software and used to identify key upstream regulators.

2.5. Statistical analyses

All statistical analyses for indices of bone microarchitecture and biomechanical testing were performed using GraphPad Prism (Version 9.5.1). Most data analysis was performed using a one-way ANOVA, $\alpha = 0.05$, followed by Tukey's post-hoc to adjust for multiple comparisons. TMD and body weight were analyzed with a non-parametric Kruskal-Wallis test, $\alpha = 0.05$, followed by Dunn's post-hoc to adjust for multiple comparisons.

3. Results

3.1. Hindlimb unloading in a young skeletally mature mouse induces an intermediate phenotype between age-matched control mice and aged mice

There were no significant differences in body weight between young control and young HLU mice (Fig. S1). After three weeks of the intervention period, there were no significant differences in cortical bone parameters in young control ($n = 8$) and young HLU (n = 8) mice (Fig. 1A-D, S2). However, both cortical area (CtAr) and tissue area (TAr) were significantly increased when comparing the aged group ($n = 11$) to either young group. Interestingly, cortical area fraction (CTAr/TAr) was significantly decreased when comparing the aged group (39 %) to young control (42.63 %, $p < 0.05$), but not to young HLU (41.50 %). There were no significant differences in cortical thickness (Ct.Th) between groups. To determine the effects of the three-week intervention period we also calculated percentage change from baseline to characterize indices of bone loss (Fig. 1E-F). From this perspective, both young control and HLU mice demonstrated a decrease in the four cortical bone indices, except for TAr, whereas aged mice demonstrated either little change or a slight increase. The HLU group was significantly different from the aged group when considering CtAr/TAr (−11.22 % vs 1.691 %, $p < 0.01$), Ct.Th (−11.39 % vs −0.5516 %, $p < 0.01$), and CtAr (−11.19 % vs 5.964 %, $p < 0.01$). There were no significant changes in TMD in male mice (Fig. S3).

Similarly, to cortical bone, indices of metaphyseal trabecular bone were not significantly different between young control and young HLU groups (Fig. 2A-D). Both young groups had lower trabecular thickness (Tb.Th) and trabecular separation (Tb.S) compared to aged controls.

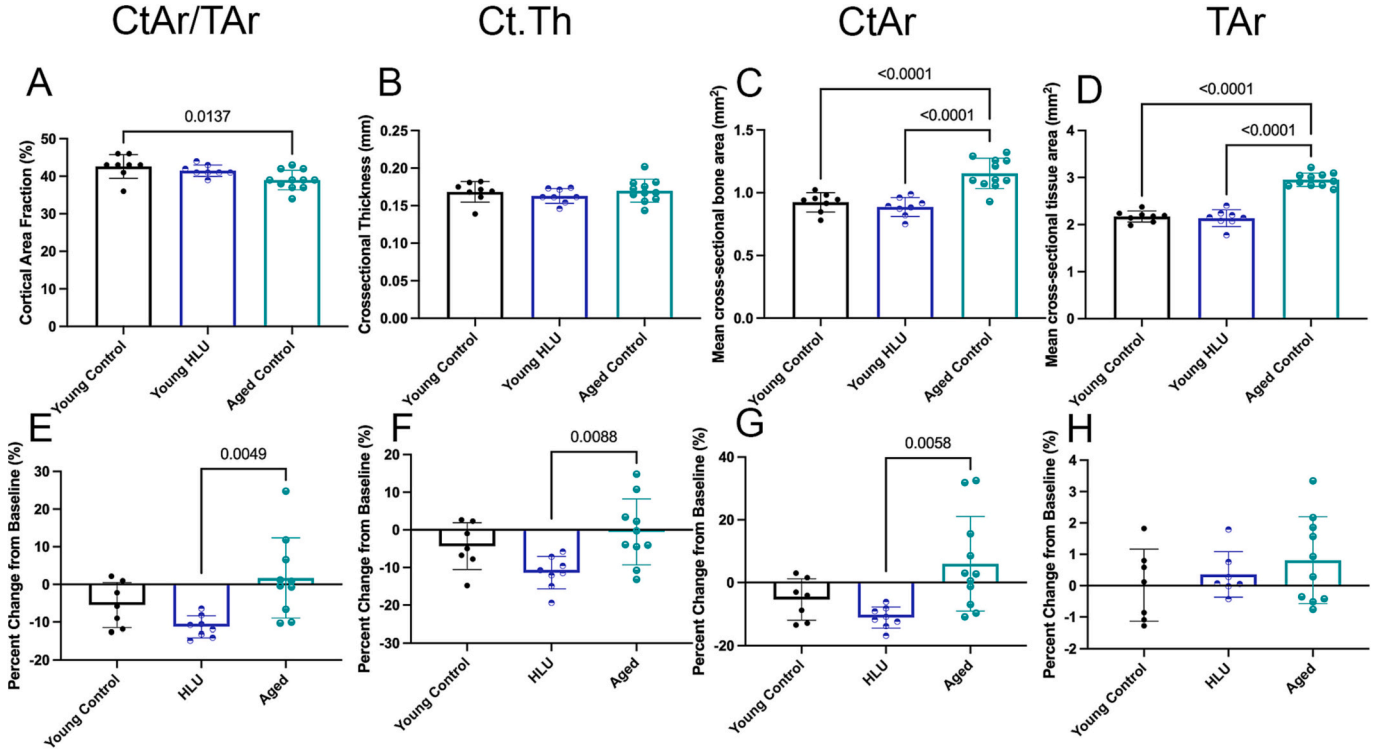

Fig. 1. Differences in cortical bone parameters in male mice after the three-week intervention period. Top: absolute values. Bottom: percent change from baseline Cortical area fraction (CtAr/TAr: A,E), cortical thickness (Ct.Th: B, F), cortical bone area (CtAr: C, G), tissue area (TAr: D, H). HLU = hind-limb unloading. Young control $n = 5$–8, young HLU $n = 6$–8, aged control, $n = 9$–11.

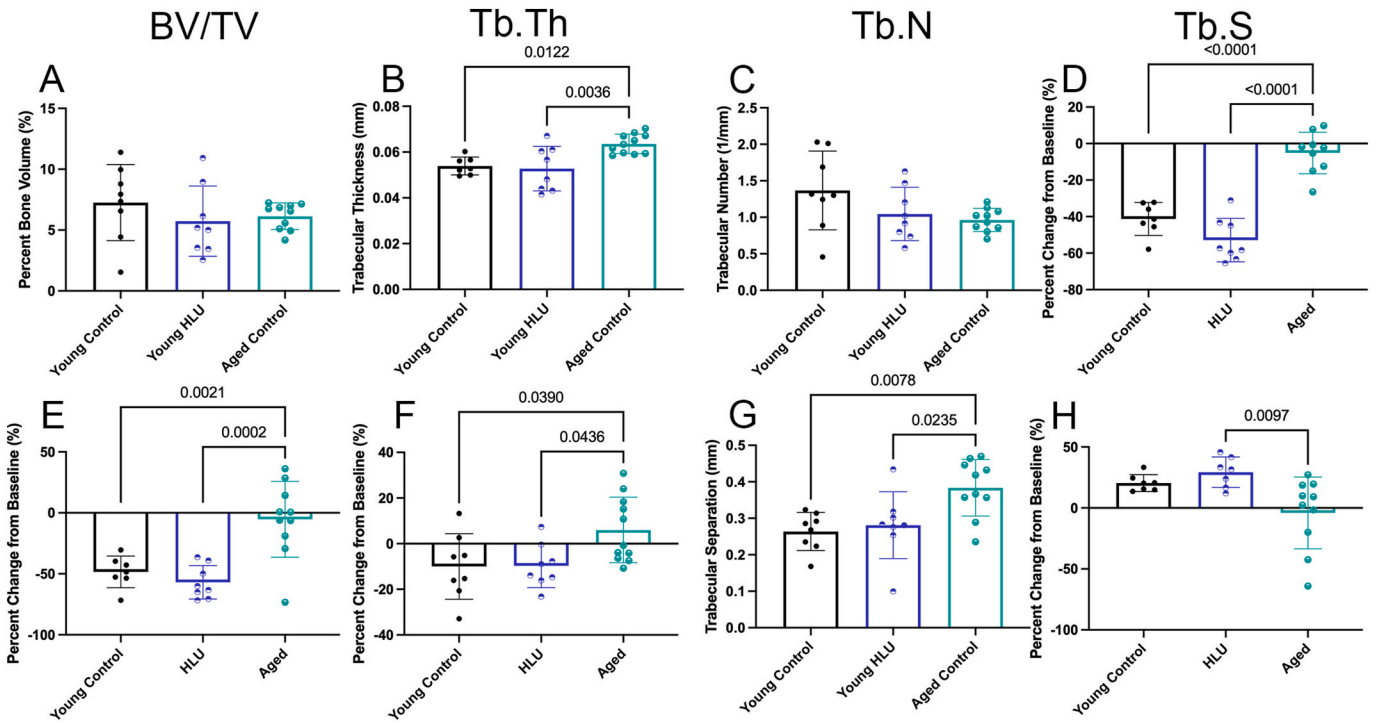

Fig. 2. Differences in metaphyseal trabecular bone parameters in male mice after the three-week intervention period. Top: absolute values. Bottom: percent change from baseline. Trabecular bone volume (BV/TV: A,E), trabecular thickness (Tb.Th: B, F), trabecular number (Tb.N: C, G), trabecular separation (Tb.S: D, H). HLU = hind-limb unloading. Young control n = 5–8, young HLU n = 6–8, aged control, n = 9–11.

However, there were no significant changes in trabecular volume (BV/TV) and trabecular number (Tb.N). In terms of change from baseline (Fig. 2E-F), BV/TV, Tb.Th and Tb.N declined in both control and HLU mice, and was significant when compared to aged mice which did not decrease as much. Tb.S increased in both control and HLU mice, but only HLU was significantly different from aged mice (+29.33 % vs −4.113 %, $p < 0.01$).

Epiphyseal trabecular bone appeared to be more susceptible to disuse than metaphyseal trabecular bone (Fig. 3A-D). There was a decrease in BV/TV and Tb.Th in the HLU group compared to the young

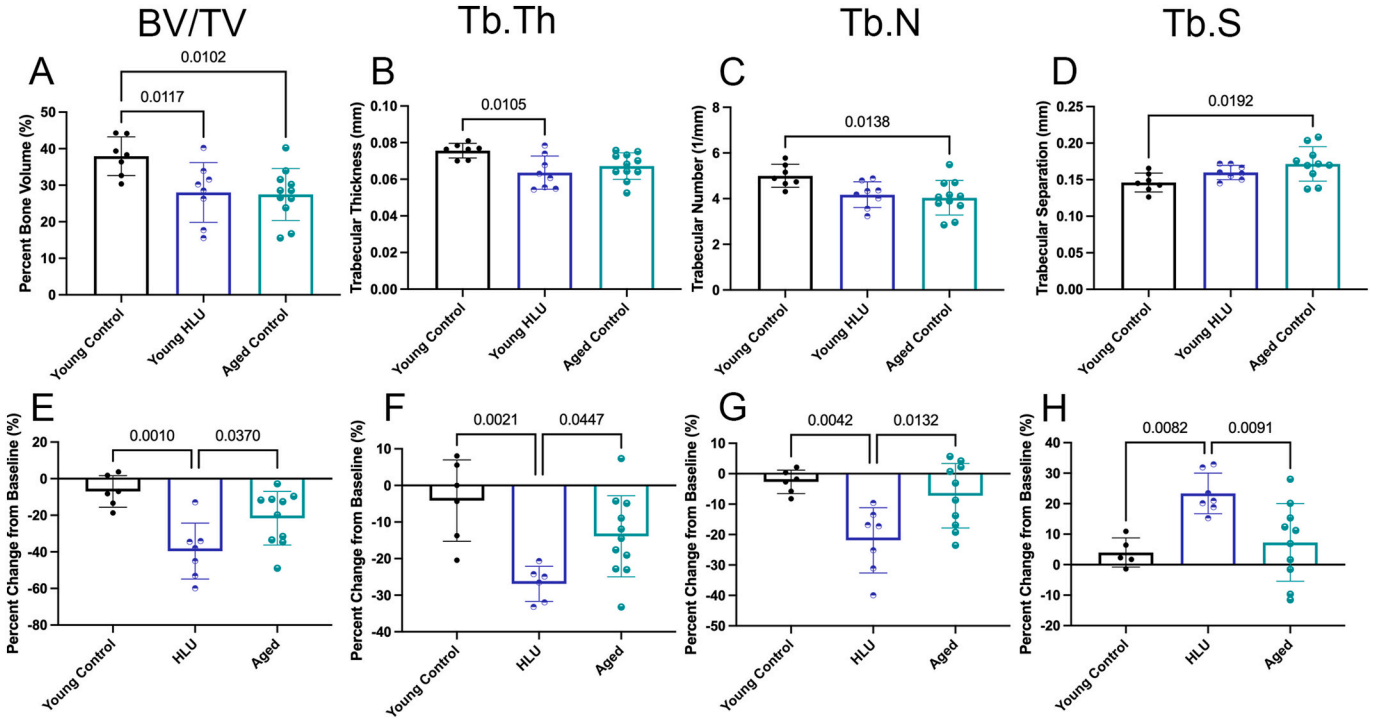

Fig. 3. Differences in epiphyseal trabecular bone parameters in male mice after the three-week intervention period. Top: absolute values. Bottom: percent change from baseline. Trabecular bone volume (BV/TV: A,E), trabecular thickness (Tb.Th: B, F), trabecular number (Tb.N: C, G), trabecular separation (Tb.S: D, H). HLU = hind-limb unloading. Young control n = 5–8, young HLU n = 6–8, aged control, n = 9–11.

control group (BV/TV: 26.94 % vs 39.93 %, $p < 0.05$, Tb.Th: 0.06362 mm vs 0.07564 mm, $p < 0.05$). There was a decrease in BV/TV and Tb.N, and an increase in Tb.S in the aged group compared to the young control group (BV/TV: 27.46 % vs 37.93 %, $p < 0.05$, Tb.N: 4.038 1/mm vs 4.999 1/mm, $p < 0.05$, Tb.S: 0.1716 mm vs 0.1462 mm, $p < 0.05$). There were no significant differences between young HLU and aged groups. Considering change from baseline (Fig. 3E-F), the young HLU demonstrated the greatest decline in BV/TV, Tb.Th and Tb.N, and increase in Tb.S. The young HLU group was significantly different compared to both young control and aged groups in all four epiphyseal trabecular bone parameters. This indicates that epiphyseal bone was the bone compartment most affected by disuse and was sufficient to accelerate the bone loss of a 6-month-old mouse to the degree of bone content to that of a 22-month-old mouse.

3.2. Femoral mechanical strength was different based on age in male mice

Three-point bending was performed on right femurs to compare bone strength between disuse and aging (Fig. 4). Aged femurs demonstrated increased yield load and ultimate load, and decreased work-to-fracture compared to either young control or young HLU. Aged femurs also demonstrated a decrease in total toughness compared to young control, but young HLU demonstrated an intermediate phenotype. There were no significant differences in post-yield deformation, yield stress, ultimate stress or post-yield strain. These findings are consistent with microarchitecture results given that the primary correlates of bone strength in three-point bending are cortical area and cortical thickness of the mid-diaphysis [27]. These findings indicate that bones in male mice are weaker with age. Disuse initiates changes in bone strength, but perhaps three weeks are not sufficient to observe large changes in mechanical strength at these age groups. In 4-month-old mice there are changes in ultimate force after HLU, but no significant changes in any other parameter [21].

3.3. Hindlimb unloading induces changes in gene expression that are age-dependent in young adult mice

After performing analysis on bone microarchitecture and biomechanical properties, we were interested in examining the gene expression profiles of each group. RNAseq was performed from marrow-flushed tibias in 4-month-old, 6-month-old and 22-month-old mice. Differential gene expression was performed and there were different patterns of gene expression induced after three weeks of HLU in 4mo and 6mo (Fig. 5). Principal component analysis was able to better separate groups based on age (Fig. 5E) rather than HLU in either 4mo or 6mo (Fig. 5A,C). Hierarchical clustering was performed to better identify the genes involved. In 4mo HLU vs control comparison, there were three main sample groupings and four gene clusters (Fig. 5B). In 6mo HLU vs control comparison, there were four main groups and two gene clusters (Fig. 5D). In 22mo vs 6mo, there were three main groups and two main gene clusters (Fig. 5F). Cluster 1 from 6mo HLU vs control and Cluster 2 in 4mo HLU vs control and 22mo vs 6mo were similar. They primarily related to muscle contraction, actin-myosin filament sliding, muscle filament sliding based on GO Biological Process 2021, and impaired skeletal muscle contractility, abnormal sarcomere morphology, abnormal muscle physiology based on MGI Mammalian Phenotype Level 42,021. These genes were highly expressed in 22mo in the 22mo vs 6mo comparison but had no clear pattern in either 4mo HLU vs Control or 6mo HLU vs Control. Cluster 4 from 4mo HLU vs Control, Cluster 2 from young HLU vs control and Cluster 1 from 22mo vs 6mo were similar. They primarily related to neutrophil mediated immunity, and more interestingly, inflammatory response and cytokine-mediated signaling pathway based on GO Biological Process 2021. MGI Mammalian Phenotype Level 42,021 ontologies relate to increased susceptibility to bacterial infection, abnormal neutrophil physiology and abnormal immune system physiology. These genes were highly expressed in 6mo HLU vs control, with no clear distinction between groups in 22mo vs 6mo or 4mo HLU vs control. These findings indicate that there are changes in gene expression with HLU that may be age-dependent early in life. However, the gene expression changes are modest compared to changes that occur with aging.

Probing further into individual candidate genes, volcano plots are displayed in Fig. 5G-I. Red dots indicate genes that are significantly upregulated in HLU or aged mice. Blue dots indicate genes that are significantly downregulated in HLU or aged mice. The threshold for significance was a logFC > |1.5| and a p-value <0.05. There are more

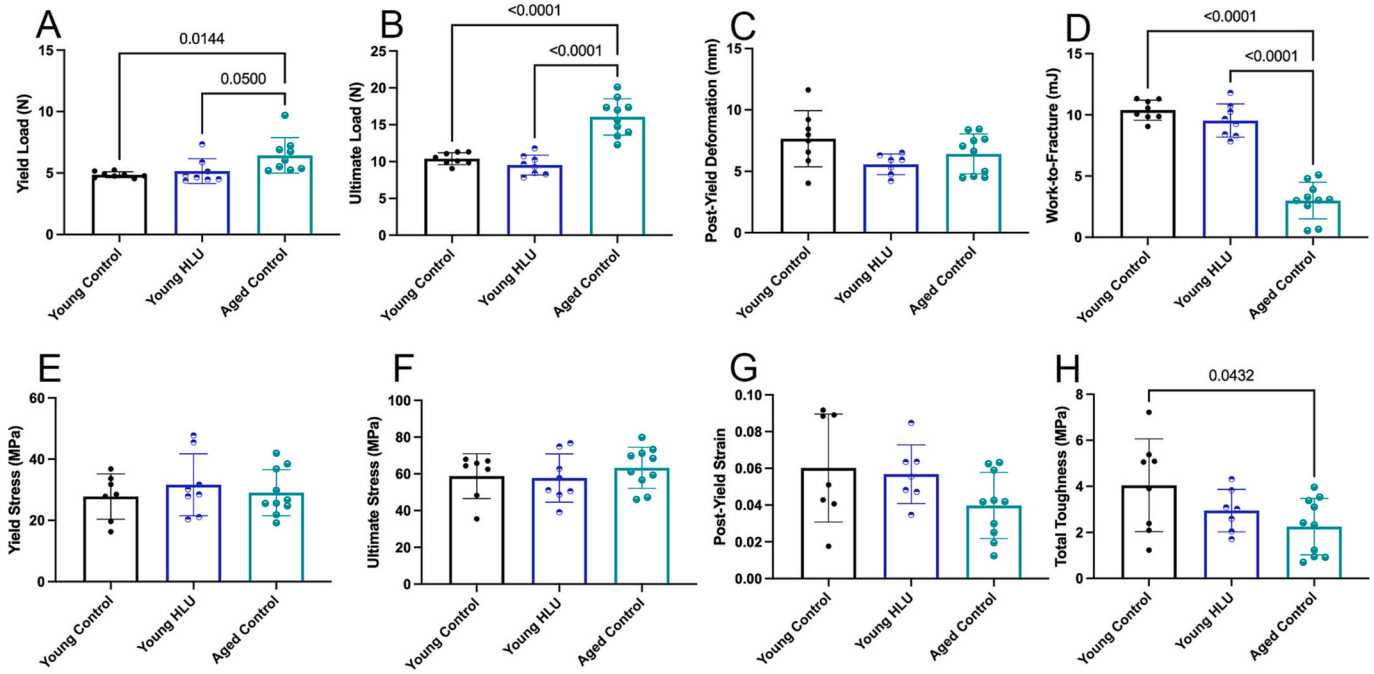

Fig. 4. Three-point bending of right femurs in male and female mice. Yield load (A), ultimate load (B), post-yield deformation (C), work-to-fracture (D), yield stress (E), ultimate stress (F), post-yield strain (G) and total toughness (H). Young control $n = 7–8$, young HLU n = 7–8, aged control, $n = 9–11$.

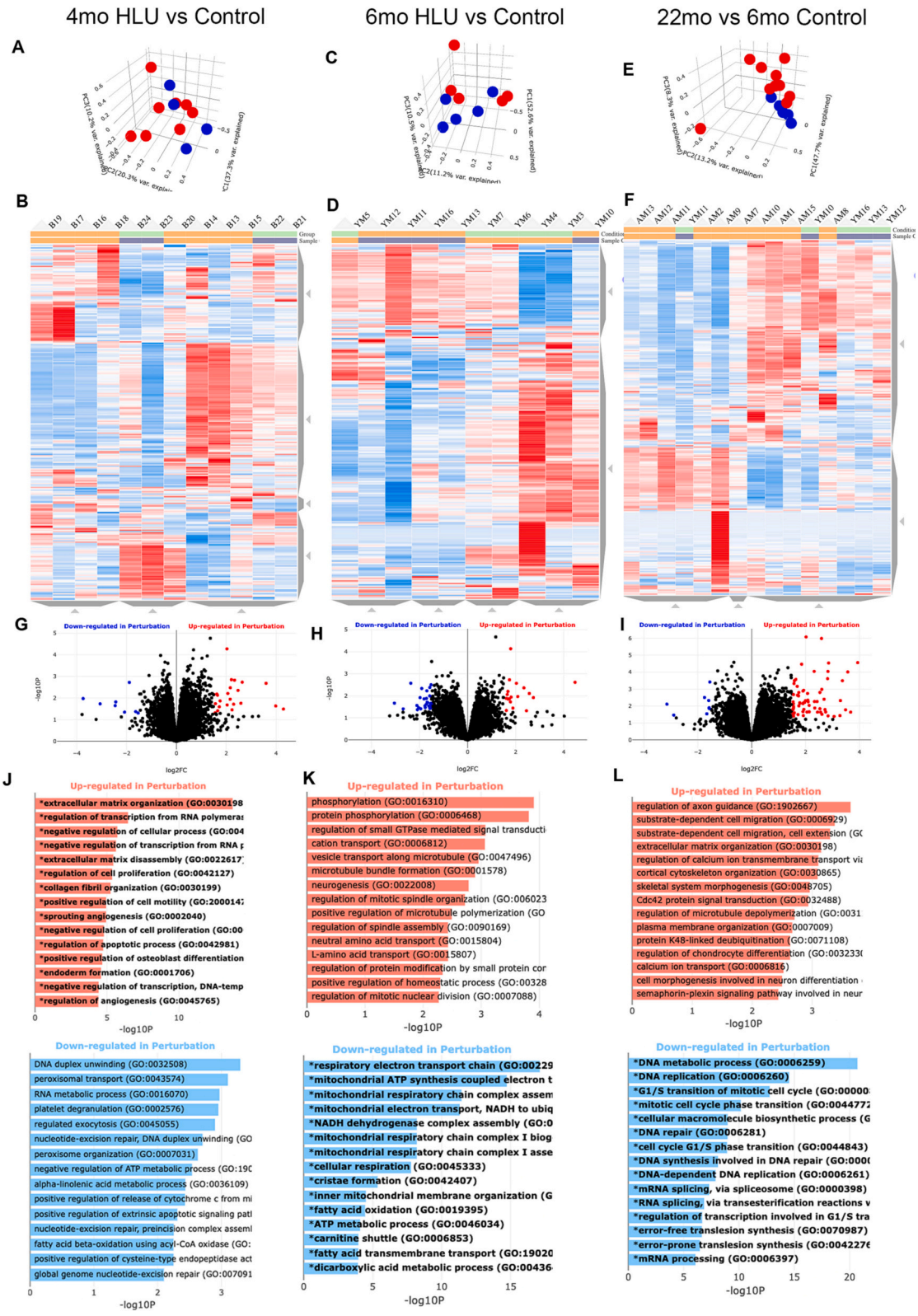

Fig. 5. Processed RNAseq data. Principal component analysis of RNAseq data comparing 4-month-old mice subject to HLU vs age-matched controls (A), 6-month-old mice subject to HLU vs age-matched controls (C), and 22-month-old mice compared to 6 month old control mice (E). Red = HLU or 22mo, Blue = Control or 6 mo, Clustergrammar of RNAseq data in each respective group. Green = HLU or 22mo, Orange = Control or 6mo (B, D,F). Volcano plot of each respective group (G, H, I). Red are significantly upregulated genes; Blue are significantly downregulated genes. logFC >1.5, $p < 0.05$. Top upregulated and downregulated pathways based on gene ontology biological processes (2018 version). Bold indicates significantly enriched pathways. (J, K, L). (For interpretation of the references to colour in this figure legend, the reader is referred to the web version of this article.)

individual upregulated genes in 22mo vs 6mo compared to both 4mo HLU vs control and 6 mo HLU vs control, this is consistent with clustergrammar (Fig. 5B.D·F) and PCA (Fig. 5A,C,E) findings. Gene ontology was performed on the top upregulated genes (Fig. 5J-L). In 4mo HLU vs control, notable ontologies include extracellular matrix organization, negative regulation of cellular process, and regulation of cell proliferation. In 6mo HLU vs control, notable ontologies include microtubule bundle formation, regulation of mitotic spindle organization, and regulation of mitotic cellular division. In 22mo vs 6mo control, notable ontologies include extracellular matrix organization, skeletal system morphogenesis, and plasma membrane organization. These results, interestingly, suggest that there is an increase in apoptosis and increased regulation of the cell cycle in response to HLU, these are characteristics also associated with age-related bone loss [3,28]. When examining the pathways related to downregulated genes, there are clues to internal cellular processes that become dysfunctional and lead to the downstream effects of each condition. In 4mo HLU vs control, notable ontologies include DNA duplex unwinding, peroxisomal transport and RNA metabolic process. In 6mo HLU vs control, notable ontologies include respiratory electron transport chain, mitochondrial ATP

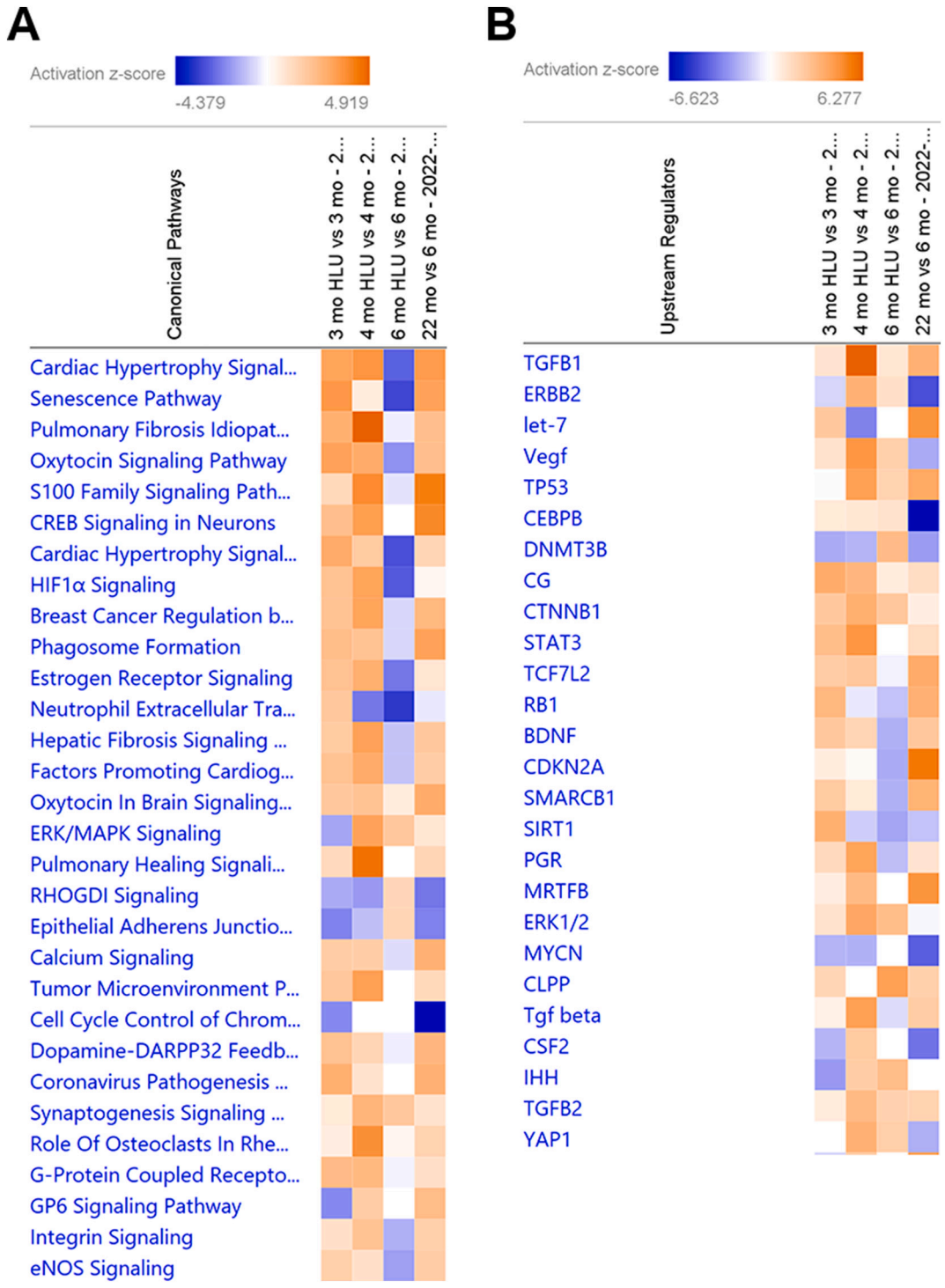

Fig. 6. Ingenuity pathway analyses of RNAseq data from HLU vs control. Comparison analysis of main canonical pathways (A) and upstream regulators (B) in HLU vs control.

synthesis coupled electron transport, and mitochondrial respiratory chain complex assembly. In 22mo vs 6mo control, notable ontologies include DNA metabolic process, DNA replication, and G1/S transition of mitotic cell cycle. These ontologies suggest that HLU might cause dysfunctional mitochondria that can perhaps lead to cellular errors in transcription and translation, whereas in aging there is primarily a downregulation of cell cycle processes. These findings with aging are expected, given the importance of senescence with aging [29]. It is also interesting considering the different findings of HLU based on age, suggesting that there may be an age-dependency to the HLU response.

To further probe this age-related response to HLU, we included additional datasets that examined HLU vs. control mice. We assessed a female dataset from 3 month old C57BL/6 mice unloaded for 7 days [26]. The gene *Klb* was significantly upregulated in 2/3 unloaded age groups, and the gene *Sptlc3* was upregulated in 2/3 unloaded age groups. *Klb* codes for Klotho beta protein, predicted to be located in the plasma membrane or endoplasmic reticulum it is thought to be involved in fibroblast growth factor signaling, upstream of the MAPKKK cascade [30,31]. *Sptlc3* is a component involved in sphingolipid biosynthesis [32]. We also compared the total list of genes significantly upregulated in any HLU group with the list of genes significantly upregulated in aging. Most interesting was *Cyp2b10* (*Cyp2b6* in humans), a component of the cytochrome P450 system, which was upregulated in 6mo HLU and aging. There were no common significantly downregulated genes in any of the groups. These gene can be potential candidates for intervention of disuse-induced bone loss and to help identify the similarities between disuse-induced bone loss and age-related bone loss.

3.4. Hindlimb unloading induced upregulation of genes involved in the senescence pathway in an age-dependent manner in young adult mice

Ingenuity pathway analysis was used to identify the leading canonical pathways and upstream regulators in each HLU age group (Fig. 6). The top five canonical pathways based on z-scored identified by IPA were “Cardiac Hypertrophy Signaling”, “Senescence Pathway”, “Pulmonary Fibrosis Idiopathic Signaling Pathway”, “Oxytocin Signaling Pathway” and “S100 Family Signaling Pathway”. IPA identified “Senescence Pathway” as the second leading canonical pathway enriched in mice exposed to HLU. HLU induced activation of the senescence pathway in 3 month ($p < 0.05$, $z = 3.464$) and 4 month ($p < 0.001$, $z = 0.6$) old mice, and inhibited it in 6 month ($p < 0.01$, $z = -3.153$) old mice. 22mo vs 6mo was included as a positive control as we hypothesized ($p < 0.0001$, $z = 3.157$). When hierarchical clustering was performed, the canonical pathways expressed by 3mo HLU vs control and 22mo vs 6mo were most similar. 4mo HLU vs control was the next most similar to this sub-grouping, whereas 6mo HLU vs control was the most distant.

The top upstream regulators in the “Genes, RNAs and Proteins” category predicted by IPA to be responsible for the pattern of gene expression were *Tgfb1, Erbb2, let-7, Vegf, Tp53 and Cebpb*. *Cebpb* encodes CCAAT/enhancer binding protein beta and is important in regulation of inflammatory gene products, including the senescence associated secretory phenotype [33,34]. IPA predicted *Cebpb* to be enriched in 3mo ($p < 0.05$, $z = 0.897$), 4mo ($p < 0.0000001$, $z = 1.032$), and 6mo ($p < 0.05$, $z = 1.427$) old mice exposed to HLU. *Erbb2* encodes erb-b2 receptor tyrosine kinase 2, a member of the epidermal growth factor family receptors and upregulation is associated with increased senescence [35]. IPA predicted *Erbb2* to be enriched in 3 month ($p < 0.05$, $z = -1.057$) and 4mo ($p < 0.0000001$, $z = 3.402$) exposed to HLU.

To determine whether changes in patterns of gene expression upon HLU were due to baseline changes in the senescence profile in age groups, IPA was performed to compare controls from each age (Fig. S4). There was activation of the senescence pathway in 4mo ($p < 0.05$, $z = 3.677$), 6mo ($p < 0.01$, $z = 2.021$) and 22mo ($p < 0.001$, $z = 1.64$) old mice relative to 3mo mice. There was similar activation of the senescence pathway in 22mo ($p < 0.0005$, $z = 3.157$) old mice relative to 6mo. Interestingly, there was decreased activation of the senescence pathway in 6mo ($p < 0.00000001$, $z = -1.606$) and 22mo ($p < 0.0000001$, $z = -0.927$) old mice relative to 4mo mice. Regarding upstream regulators, *Cebpb* ($p < 0.00000001$, $z = -6.623$) and *Erbb2* ($p < 0.00000001$, $z = -4.548$) were predicted to decrease in 22mo mice relative to 6mo mice, whereas *Cdkn2a* ($p < 0.00000001$, $z = 5.487$) was predicted to increase. In summary, in response to HLU in 3mo and 4mo mice the pattern of activation or inhibition of the most enriched canonical pathways and upstream regulators appeared to imitate the pattern in response to aging. However, this pattern was the opposite to the response to HLU in 6mo and 22mo mice. This suggests that there may be an age-dependent response to HLU in young adult mice.

Ingenuity pathway analysis was also used to generate summary graphics for each HLU vs control age group comparison and the aged vs young comparison (Fig. S5). Centrally located nodes have a higher number of connections than distally located nodes. In 3mo HLU vs control, there are genes related to a viral response. In 4mo HLU vs control, there are genes related to inflammatory cytokines *Il6, Il1b, Tnfsf11, Tgb1, Pdgfc* and their activated pathways *Stat3, Ikbkb, Smad3*, *Src*. There are also molecules involved in cellular proliferation and wound healing *Bmp2, Egf, Vegfa, Wnt1*. In 6mo HLU vs control, the central genes being influenced are *Ppargc1a* and *Pnpla2*, leading to dysfunction in energy homeostasis, consumption of oxygen and energy expenditure. The predicted disease states are glucose metabolism disorder and obesity. In 22mo mice vs 6mo mice, the central components of the interaction pathway relate to *Tp53, Cdkn2a*, *Rbl1* and Cell cycle: G2/M DNA damage checkpoint regulation. This variability in response to HLU in each age group suggests that there may be age-related differences after HLU in terms of the pathway leading to disuse-induced bone loss.

4. Discussion

Our hypothesis was based on the idea that age- and disuse-related bone loss shared a similar phenotype. In this study, we demonstrated that a disuse condition such as hindlimb unloading over a three-week period initiates several changes in bone microarchitecture and gene expression that are similar to aging. Both aging [34–36] and disuse [18,36–38] demonstrate RANKL-dependent increased osteoclast bone resorption, decreased osteoblast bone formation and osteocyte apoptosis [3]. Although a major difference is that bone turnover is increased with disuse [39], whereas remodeling is decreased with aging [40]. It should be noted that a three-week period of unloading is likely insufficient to develop permanent changes in tissue when compared to the numerous cellular, tissue and organ level changes that occur with aging. In fact, younger mice are able to recover bone after a period of reambulation [5,41]. It would be interesting to explore longer periods of disuse to determine if there is a critical turning point, whereby permanent changes cannot be rescued, or if such a period is solely dependent on age.

This study compared the microarchitecture, biomechanical properties, and gene expression of young, unloaded, and aged mice to identify similarities and differences. Trabecular bone compartments were more influenced by unloading than aging. This is interesting, considering that on visual inspection of microCT images there appears to be less trabeculae with aging, but this is not reflected on calculation (Figs. 2,3, S2). It is possible that software used to calculate trabecular bone volume was not able to accurately parse bone signals from background in aged mice due to the lack of trabeculae. Alternatively, the 7 μm voxel size that we used may not be sufficient resolution to observe the presence of thin trabeculae, at which point, nanoCT may be required to visualize changes. Trabecular bone is important for transmitting forces throughout the anatomy of the bone, and so it would logically decrease in the context of disuse [42,43]. However, previous studies have also indicated decreases in trabecular bone volume with age [44]. In terms of biomechanical strength testing, our male mice demonstrated an increase

in ultimate load and decrease in work to fracture with aging, but no change after disuse. This is consistent with previous findings, where most of the variability in biomechanical strength is correlated with cortical bone parameters such as cortical fraction and cortical thickness [45,46]. In summary, it appears that aging and disuse both result in bone loss in the femur, but with emphasis on different areas of the femur.

Gene expression results indicated that aging causes more transcriptome level changes than disuse. Our results indicate that aged mice already have significant defects in cell cycle processes, increased inflammation, and increased senescence. The cellular changes observed in disuse, particularly in regard to mitochondrial dysfunction and errors in the electron transport chain, are some signature features of senescence [47–49]. They can lead to increases in reactive oxygen species and activate senescence pathways [40,50]. Others have suggested that simulated microgravity in vitro induces senescence via mitochondrial dysfunction and oxidative stress in mesenchymal stem cells [51], skeletal muscle myoblasts [52], and neural crest-derived rat pheochromocytoma cells [53]. However, it should be noted that our model of disuse only occurred over three weeks. Senescence develops as a result of long-term chronic stress/insults, so it is possible that these observed changes are only early stages of dysfunction that can lead to senescence or apoptosis [7]. This might inform preventive strategies depending on timing of disuse. Perhaps prophylactic measures to prevent disuse-related bone loss should focus on mitigating mitochondrial dysfunction and oxidative stress, whereas chronic exposure may require a dual-treatment strategy against senescent cells and the SASP.

These data indicate that there is an age-dependent change in activation of the senescence pathway upon HLU in young adult mice (3–4 months), but not in slightly older mice (6 months). This work demonstrates that both aging and disuse upregulate the senescence pathway, but do not completely overlap. It is unclear why 4mo mice demonstrated the highest activation of the senescence pathway among the age groups in control mice. This time period coincides with peak bone mineral density and volume in C57BL/6 mice, after which there is a decline in cortical and trabecular bone architecture with increasing age [44]. It is possible that this arrest in gross bone growth coincides with a physiologic induction of senescence as observed during periods of embryonic development and wound healing [29,54]. A potential confounding factor is our model of disuse; hindlimb unloading. There are concerns that this model can increase the amount of inflammatory cytokines and induce a stress response [55], although one study notes that the stress response is more related to social isolation rather than physiological stress [56]. Given these concerns, it would be interesting to compare these findings using alternative models of disuse, albeit with their own drawbacks, such as sciatic neurectomy [57], single-limb immobilization [58] or cage-restricted movement [59]. Nevertheless, these results will need to be experimentally validated to identify a mechanism that links mechanical stimuli to mitochondrial function.

It should be noted that only male mice were used in this study, except for the inclusion of GSE169292 in IPA. There are additional differences that should be considered when comparing the results of GS169292 to our study. This dataset used 3-month-old C57BL/6 N female mice that were subjected to HLU for a period of 7 days, whereas our studies used C57BL/6 J mice subjected to HLU for a period of 3 weeks. Regardless, it is interesting that this dataset displayed a similar pattern of response to HLU when compared to our 4-month-old male mice (Fig. 6), suggesting that the HLU response may really change depending on age. However, relationships in bone microarchitecture and biomechanical properties may be expressed differently in female mice, and that was not explored in this study. Female mice will need to be examined at these age groups to determine if there are sex-dependent effects when comparing disuse- and age-related bone loss [44,45].

Our study has additional limitations. Foremost, gene expression data from RNAseq will need to be validated through alternative techniques including qPCR, Western blot, ELISA and/or histology from a new set of biological replicates. This is important to detect changes in certain genes of interest such as *Cdkn1a*, *Cdkn2a*, *Cebpb*, *Erbb2*, and *Klb*. Further, bone microarchitecture and biomechanical properties were examined in femurs, while gene expression was examined in tibiae. Although similar changes occur in both femur and tibiae after disuse [60], it is possible that cellular responses are different. On another note, to better test the effect of aging it would have been optimal to perform a longitudinal study beginning at 6-months of age. This would have allowed us to better characterize the bone microarchitecture changes during aging since mice at 6-months and 22-months would serve as internal controls. Lastly, it is important to consider confounding effects of our disuse model. Regardless, our study provides insight into the changes that may be similar or different in response to age- and disuse-related bone loss.

Our results suggest that disuse may establish a senescent phenotype in young adult long bones. This has implications for young individuals who experience extended periods of disuse as would occur from lack of exercise, bedrest, limb immobilization and spinal cord injury. It also suggests that senolytics, drugs that selectively eliminate senescent cells, may be a future strategy to prevent disuse-induced bone loss in young adult long bones.

Contributions

Conceptualization: SJM, MAF, JNF, HJD.
Methodology: SJM, MAF, PG, JNF, HJD.
Investigation: SJM, GMD, RD.
Analysis: SJM, GMD, MAF, RD, PG, HJD.
Writing and Editing: SJM, GMD, MAF, RD, PG, JNF, HJD.

CRediT authorship contribution statement

Steven J. Meas: Writing – review & editing, Writing – original draft, Visualization, Validation, Methodology, Investigation, Funding acquisition, Formal analysis, Data curation, Conceptualization. **Gabriella M. Daire:** Writing – review & editing, Writing – original draft, Visualization, Investigation, Formal analysis. **Michael A. Friedman:** Writing – review & editing, Writing – original draft, Supervision, Methodology, Formal analysis, Conceptualization. **Rachel DeNapoli:** Writing – review & editing, Investigation, Formal analysis. **Preetam Ghosh:** Writing – review & editing, Methodology, Formal analysis, Data curation. **Joshua N. Farr:** Writing – review & editing, Supervision, Methodology, Conceptualization. **Henry J. Donahue:** Writing – review & editing, Writing – original draft, Supervision, Resources, Project administration, Methodology, Funding acquisition, Data curation, Conceptualization.

Declaration of competing interest

The authors have no conflicts of interest to disclose.

Data availability

RNAseq raw and processed files have been uploaded to GEO and are available under the following accession number: GSE235942.

Acknowledgments

This work was funded by NIH R01 AR068132, NASA 80NSSC18K1473, and CIHR DFSA 454761. We would like to thank the VCU Genomics Core for their assistance in performing RNAseq library preparation and sequencing.

Appendix A. Supplementary data

Supplementary data to this article can be found online at https://doi.org/10.1016/j.bone.2023.116973.

References

[1] M.A. Clynes, N.C. Harvey, E.M. Curtis, N.R. Fuggle, E.M. Dennison, C. Cooper, The epidemiology of osteoporosis, Br. Med. Bull. 133 (2020) 105–117, https://doi.org/10.1093/bmb/ldaa005.

[2] S.R. Cummings, L.J. Melton, Epidemiology and outcomes of osteoporotic fractures, Lancet (London, England). 359 (2002) 1761–1767, https://doi.org/10.1016/S0140-6736(02)08657-9.

[3] E.G. Buettmann, G.M. Goldscheitter, G.A. Hoppock, M.A. Friedman, L.J. Suva, H. J. Donahue, Similarities between disuse and age-induced bone loss, journal of bone and mineral research, The Official Journal of the American Society for Bone and Mineral Research. 37 (2022) 1417–1434, https://doi.org/10.1002/jbmr.4643.

[4] L. Vico, A. Hargens, Skeletal changes during and after spaceflight, nature reviews, Rheumatology 14 (2018) 229–245, https://doi.org/10.1038/nrrheum.2018.37.

[5] H.C. Cunningham, D.W.D. West, L.M. Baehr, F.D. Tarke, K. Baar, S.C. Bodine, et al., Age-dependent bone loss and recovery during hindlimb unloading and subsequent reloading in rats, BMC Musculoskelet. Disord. 19 (2018) 223, https://doi.org/10.1186/s12891-018-2156-x.

[6] L. Bonewald, Use it or lose it to age: a review of bone and muscle communication, Bone 120 (2019) 212–218, https://doi.org/10.1016/j.bone.2018.11.002.

[7] S. Khosla, J.N. Farr, D.G. Monroe, Cellular senescence and the skeleton: pathophysiology and therapeutic implications, J. Clin. Invest. 132 (2022), https://doi.org/10.1172/JCI154888.

[8] J.N. Farr, D.G. Fraser, H. Wang, K. Jaehn, M.B. Ogrodnik, M.M. Weivoda, et al., Identification of senescent cells in the bone microenvironment, journal of bone and mineral research, The Official Journal of the American Society for Bone and Mineral Research. 31 (2016) 1920–1929, https://doi.org/10.1002/jbmr.2892.

[9] J.N. Farr, M. Xu, M.M. Weivoda, D.G. Monroe, D.G. Fraser, J.L. Onken, et al., Targeting cellular senescence prevents age-related bone loss in mice, Nat. Med. 23 (2017) 1072–1079, https://doi.org/10.1038/nm.4385.

[10] J.N. Farr, J. Kaur, M.L. Doolittle, S. Khosla, Osteocyte Cellular Senescence, Curr. Osteoporos. Rep. 18 (2020) 559–567, https://doi.org/10.1007/s11914-020-00619-x.

[11] H.-N. Kim, J. Chang, S. Iyer, L. Han, J. Campisi, S.C. Manolagas, et al., Elimination of senescent osteoclast progenitors has no effect on the age-associated loss of bone mass in mice, Aging Cell 18 (2019), e12923, https://doi.org/10.1111/acel.12923.

[12] C.E. Metzger, S. Anand Narayanan, P.H. Phan, S.A. Bloomfield, Hindlimb unloading causes regional loading-dependent changes in osteocyte inflammatory cytokines that are modulated by exogenous irisin treatment, NPJ Microgravity. 6 (2020) 28, https://doi.org/10.1038/s41526-020-00118-4.

[13] M. Yakabe, S. Ogawa, H. Ota, K. Iijima, M. Eto, Y. Ouchi, et al., Inhibition of interleukin-6 decreases atrogene expression and ameliorates tail suspension-induced skeletal muscle atrophy, PloS One 13 (2018), e0191318, https://doi.org/10.1371/journal.pone.0191318.

[14] P. Lau, L. Vico, J. Rittweger, Dissociation of bone resorption and formation in spaceflight and simulated microgravity: potential role of Myokines and Osteokines? Biomedicines 10 (2022) https://doi.org/10.3390/biomedicines10020342.

[15] H. Che, J. Li, Y. Li, C. Ma, H. Liu, J. Qin, et al., p16 deficiency attenuates intervertebral disc degeneration by adjusting oxidative stress and nucleus pulposus cell cycle, eLife 9 (2020), https://doi.org/10.7554/eLife.52570.

[16] E.J. Novais, B.O. Diekman, I.M. Shapiro, M.V. Risbud, p16Ink4a deletion in cells of the intervertebral disc affects their matrix homeostasis and senescence associated secretory phenotype without altering onset of senescence, Matrix Biol. 82 (2019) 54–70, https://doi.org/10.1016/j.matbio.2019.02.004.

[17] M.A. Friedman, Y. Zhang, J.S. Wayne, C.R. Farber, H.J. Donahue, Single limb immobilization model for bone loss from unloading, J. Biomech. 83 (2019) 181–189, https://doi.org/10.1016/j.jbiomech.2018.11.049.

[18] S.A. Lloyd, G.S. Lewis, Y. Zhang, E.M. Paul, H.J. Donahue, Connexin 43 deficiency attenuates loss of trabecular bone and prevents suppression of cortical bone formation during unloading, journal of bone and mineral research, The Official Journal of the American Society for Bone and Mineral Research. 27 (2012) 2359–2372, https://doi.org/10.1002/jbmr.1687.

[19] S.J. Jackson, N. Andrews, D. Ball, I. Bellantuono, J. Gray, L. Hachoumi, et al., Does age matter? The impact of rodent age on study outcomes, Laboratory Animals 51 (2017) 160–169, https://doi.org/10.1177/0023677216653984.

[20] E.G. Buettmann, R.C. DeNapoli, L.B. Abraham, J.A. Denisco, M.R. Lorenz, M. A. Friedman, et al., Reambulation following hindlimb unloading attenuates disuse-induced changes in murine fracture healing, Bone 172 (2023), 116748, https://doi.org/10.1016/j.bone.2023.116748.

[21] M.A. Friedman, E.G. Buettmann, Y. Zeineddine, L.B. Abraham, G.A. Hoppock, S. J. Meas, et al., Genetic variation influences the skeletal response to Hindlimb unloading in the eight founder strains of the diversity outbred mouse population, J. Orthop. Res. (2023), https://doi.org/10.1002/jor.25646.

[22] D. Torre, A. Lachmann, A. Ma'ayan, BioJupies: automated generation of interactive notebooks for RNA-Seq data analysis in the cloud, Cell Syst. 7 (2018) 556–561.e3, https://doi.org/10.1016/j.cels.2018.10.007.

[23] N.F. Fernandez, G.W. Gundersen, A. Rahman, M.L. Grimes, K. Rikova, P. Hornbeck, et al., Clustergrammer, a web-based heatmap visualization and analysis tool for high-dimensional biological data, Scientific Data. 4 (2017), 170151, https://doi.org/10.1038/sdata.2017.151.

[24] M.E. Ritchie, B. Phipson, D. Wu, Y. Hu, C.W. Law, W. Shi, et al., Limma powers differential expression analyses for RNA-sequencing and microarray studies, Nucleic Acids Res. 43 (2015), e47, https://doi.org/10.1093/nar/gkv007.

[25] A. Krämer, J. Green, J. Pollard, S. Tugendreich, Causal analysis approaches in ingenuity pathway analysis, Bioinformatics (Oxford, England). 30 (2014) 523–530, https://doi.org/10.1093/bioinformatics/btt703.

[26] J.M. Spatz, F.C. Ko, U.M. Ayturk, M.L. Warman, M.L. Bouxsein, RNAseq and RNA molecular barcoding reveal differential gene expression in cortical bone following hindlimb unloading in female mice, PloS One 16 (2021), e0250715, https://doi.org/10.1371/journal.pone.0250715.

[27] N. Migotsky, M.D. Brodt, J.M. Cheverud, M.J. Silva, Cortical bone relationships are maintained regardless of sex and diet in a large population of LGXSM advanced intercross mice, Bone Reports. 17 (2022), 101615, https://doi.org/10.1016/j.bonr.2022.101615.

[28] R.J. Pignolo, S.F. Law, A. Chandra, Bone Aging, Cellular Senescence, and Osteoporosis, JBMR Plus. 5 (2021), e10488, https://doi.org/10.1002/jbm4.10488.

[29] S. He, N.E. Sharpless, Senescence in health and disease, Cell 169 (2017) 1000–1011, https://doi.org/10.1016/j.cell.2017.05.015.

[30] X. Li, The FGF metabolic axis, Frontiers of Medicine. 13 (2019) 511–530, https://doi.org/10.1007/s11684-019-0711-y.

[31] G.J. Prud'homme, M. Kurt, Q. Wang, Pathobiology of the klotho antiaging protein and therapeutic considerations, Front Aging. 3 (2022), 931331, https://doi.org/10.3389/fragi.2022.931331.

[32] M. Trayssac, Y.A. Hannun, L.M. Obeid, Role of sphingolipids in senescence: implication in aging and age-related diseases, J. Clin. Invest. 128 (2018) 2702–2712, https://doi.org/10.1172/JCI97949.

[33] T. Sebastian, R. Malik, S. Thomas, J. Sage, P.F. Johnson, C/EBPbeta cooperates with RB:E2F to implement Ras(V12)-induced cellular senescence, EMBO J. 24 (2005) 3301–3312, https://doi.org/10.1038/sj.emboj.7600789.

[34] T. Kuilman, C. Michaloglou, L.C.W. Vredeveld, S. Douma, R. van Doorn, C. J. Desmet, et al., Oncogene-induced senescence relayed by an interleukin-dependent inflammatory network, Cell 133 (2008) 1019–1031, https://doi.org/10.1016/j.cell.2008.03.039.

[35] P.D. Angelini, M.F. Zacarias Fluck, K. Pedersen, J.L. Parra-Palau, M. Guiu, C. Bernadó Morales, et al., Constitutive HER2 signaling promotes breast cancer metastasis through cellular senescence, Cancer Res. 73 (2013) 450–458, https://doi.org/10.1158/0008-5472.CAN-12-2301.

[36] E.A. Blaber, N. Dvorochkin, C. Lee, J.S. Alwood, R. Yousuf, P. Pianetta, et al., Microgravity induces pelvic bone loss through osteoclastic activity, osteocytic osteolysis, and osteoblastic cell cycle inhibition by CDKN1a/p21, PloS One 8 (2013), e61372, https://doi.org/10.1371/journal.pone.0061372.

[37] J.I. Aguirre, L.I. Plotkin, S.A. Stewart, R.S. Weinstein, A.M. Parfitt, S.C. Manolagas, et al., Osteocyte apoptosis is induced by weightlessness in mice and precedes osteoclast recruitment and bone loss, journal of bone and mineral research, The Official Journal of the American Society for Bone and Mineral Research. 21 (2006) 605–615, https://doi.org/10.1359/jbmr.060107.

[38] P. Cabahug-Zuckerman, D. Frikha-Benayed, R.J. Majeska, A. Tuthill, S. Yakar, S. Judex, et al., Osteocyte apoptosis caused by Hindlimb unloading is required to trigger osteocyte RANKL production and subsequent resorption of cortical and trabecular bone in mice femurs, journal of bone and mineral research, The Official Journal of the American Society for Bone and Mineral Research. 31 (2016) 1356–1365, https://doi.org/10.1002/jbmr.2807.

[39] S.A. Lloyd, A.E. Loiselle, Y. Zhang, H.J. Donahue, Connexin 43 deficiency desensitizes bone to the effects of mechanical unloading through modulation of both arms of bone remodeling, Bone 57 (2013) 76–83, https://doi.org/10.1016/j.bone.2013.07.022.

[40] M. Almeida, L. Han, M. Martin-Millan, L.I. Plotkin, S.A. Stewart, P.K. Roberson, et al., Skeletal involution by age-associated oxidative stress and its acceleration by loss of sex steroids, J. Biol. Chem. 282 (2007) 27285–27297, https://doi.org/10.1074/jbc.M702810200.

[41] H.C. Cunningham, S. Orr, D.K. Murugesh, A.W. Hsia, B. Osipov, L. Go, et al., Differential bone adaptation to mechanical unloading and reloading in young, old, and osteocyte deficient mice, Bone 167 (2023), 116646, https://doi.org/10.1016/j.bone.2022.116646.

[42] E. Ozcivici, S. Judex, Trabecular bone recovers from mechanical unloading primarily by restoring its mechanical function rather than its morphology, Bone 67 (2014) 122–129, https://doi.org/10.1016/j.bone.2014.05.009.

[43] J. Ozawa, A. Kaneguchi, S. Ezumi, T. Maeno, J. Iwazawa, K. Minanimoto, et al., Effects of hindlimb suspension on development of proximal and distal femur morphological abnormalities in growing rats, Journal of Orthopaedic Research: Official Publication of the Orthopaedic Research Society. 41 (2023) 364–377, https://doi.org/10.1002/jor.25352.

[44] V. Glatt, E. Canalis, L. Stadmeyer, M.L. Bouxsein, Age-related changes in trabecular architecture differ in female and male C57BL/6J mice, journal of bone and mineral research, The Official Journal of the American Society for Bone and Mineral Research. 22 (2007) 1197–1207, https://doi.org/10.1359/jbmr.070507.

[45] M.D. Willinghamm, M.D. Brodt, K.L. Lee, A.L. Stephens, J. Ye, M.J. Silva, Age-related changes in bone structure and strength in female and male BALB/c mice, Calcif. Tissue Int. 86 (2010) 470–483, https://doi.org/10.1007/s00223-010-9359-y.

[46] M.D. Brodt, C.B. Ellis, M.J. Silva, Growing C57Bl/6 mice increase whole bone mechanical properties by increasing geometric and material properties, journal of bone and mineral research, The Official Journal of the American Society for Bone and Mineral Research. 14 (1999) 2159–2166, https://doi.org/10.1359/jbmr.1999.14.12.2159.

[47] S.R. Kim, A. Eirin, X. Zhang, A. Lerman, L.O. Lerman, Mitochondrial protection partly mitigates kidney cellular senescence in swine atherosclerotic renal artery stenosis, Cell. Physiol. Biochem. 52 (2019) 617–632, https://doi.org/10.33594/000000044.

[48] C. Zhang, S. Xu, S. Zhang, M. Liu, H. Du, R. Sun, et al., Ageing characteristics of bone indicated by transcriptomic and exosomal proteomic analysis of cortical bone cells, J. Orthop. Surg. Res. 14 (2019) 129, https://doi.org/10.1186/s13018-019-1163-4.
[49] V. Moiseeva, A. Cisneros, V. Sica, O. Deryagin, Y. Lai, S. Jung, et al., Senescence atlas reveals an aged-like inflamed niche that blunts muscle regeneration, Nature 613 (2023) 169–178, https://doi.org/10.1038/s41586-022-05535-x.
[50] C. Correia-Melo, F.D.M. Marques, R. Anderson, G. Hewitt, R. Hewitt, J. Cole, et al., Mitochondria are required for pro-ageing features of the senescent phenotype, EMBO J. 35 (2016) 724–742, https://doi.org/10.15252/embj.201592862.
[51] W. Lv, X. Peng, Y. Tu, Y. Shi, G. Song, Q. Luo, YAP inhibition alleviates simulated microgravity-induced mesenchymal stem cell senescence via targeting mitochondrial dysfunction, Antioxidants (Basel). 12 (2023) 990, https://doi.org/10.3390/antiox12050990.
[52] H. Takahashi, A. Nakamura, T. Shimizu, Simulated microgravity accelerates aging of human skeletal muscle myoblasts at the single cell level, Biochem. Biophys. Res. Commun. 578 (2021) 115–121, https://doi.org/10.1016/j.bbrc.2021.09.037.
[53] F.-S. Wang, R.-W. Wu, Y.-S. Chen, J.-Y. Ko, H. Jahr, W.-S. Lian, Biophysical modulation of the mitochondrial metabolism and redox in bone homeostasis and osteoporosis: how biophysics converts into bioenergetics, Antioxidants (Basel). 10 (2021), https://doi.org/10.3390/antiox10091394.
[54] S. Khosla, Senescent cells, senolytics and tissue repair: the devil may be in the dosing, Nat. Aging. (2023) 1–3, https://doi.org/10.1038/s43587-023-00365-6.
[55] L. Kutz, T. Zhou, Q. Chen, H. Zhu, A Surgical Approach to Hindlimb Suspension: A Mouse Model of Disuse-Induced Atrophy, Methods in Molecular Biology (Clifton, N.J.). 2597 (2023) 1–9. doi:https://doi.org/10.1007/978-1-0716-2835-5_1.
[56] A.A. Naumova, E.A. Oleynik, Y.S. Grigorieva, S.D. Nikolaeva, E.V. Chernigovskaya, M.V. Glazova, In search of stress: analysis of stress-related markers in mice after hindlimb unloading and social isolation, Neurol. Res. 45 (2023) 957–968, https://doi.org/10.1080/01616412.2023.2252280.
[57] S. Monzem, B. Javaheri, R.L. de Souza, A.A. Pitsillides, Sciatic neurectomy-related cortical bone loss exhibits delayed onset yet stabilises more rapidly than trabecular bone, Bone Reports. 15 (2021), 101116, https://doi.org/10.1016/j.bonr.2021.101116.
[58] M.A. Friedman, A. Abood, B. Senwar, Y. Zhang, C.R. Maroni, V.L. Ferguson, et al., Genetic variability affects the skeletal response to immobilization in founder strains of the diversity outbred mouse population, Bone Reports. 15 (2021), 101140, https://doi.org/10.1016/j.bonr.2021.101140.
[59] P. Roemers, Y. Hulst, S. van Heijningen, G. van Dijk, M.J.G. van Heuvelen, P.P. De Deyn, et al., Inducing physical inactivity in mice: preventing climbing and reducing cage size negatively affect physical fitness and body composition, Front. Behav. Neurosci. 13 (2019) 221, https://doi.org/10.3389/fnbeh.2019.00221.
[60] A.R. Krause, T.A. Speacht, J.L. Steiner, C.H. Lang, H.J. Donahue, Mechanical loading recovers bone but not muscle lost during unloading, NPJ Microgravity. 6 (2020) 36, https://doi.org/10.1038/s41526-020-00126-4.